DOI: 10.2478/eces-2026-0004 ECOL CHEM ENG S. 2026;33(1):63-79

Safa MOHAMMED[1] and Basma WAISI[1*]

STRUCTURE-PERFORMANCE ENGINEERING OF RECYCLED ACRYLIC MEMBRANES FOR AIR GAP MEMBRANE DISTILLATION

Abstract: Air Gap Membrane Distillation (AGMD) is an emerging and promising technology in separation processes, but its industrial adoption is limited by relatively low permeate flux. Conventional AGMD systems typically utilise thin film-cast polymeric membranes. However, electrospun nanofibrous membranes have become more popular since they possess a highly interconnected porous structure, which is able to increase mass transfer performance and availability. In this study, recycled acrylic (RA) waste powder was used to prepare a precursor solution to fabricate two types of membranes: thin film-cast membranes and electrospun nonwoven nanofibrous membranes to be evaluated in the AGMD process for water desalination application. The fabricated RA-based membranes underwent characterisation by scanning electronic microscopy (SEM), mechanical properties, water contact angle (WCA), and Fourier transform infrared spectroscopy (FTIR). Based on the results obtained, the nanofiber membrane exhibited a higher contact angle, porosity, and elasticity than the thin film cast membrane. RA-based membranes were tested in the AGMD system at different feed temperatures (45 °C, 55 °C, and 65 °C). The electrospun nanofibrous membrane performed better than the thin-film cast membrane in both permeate flux and salt rejection. The temperature of the feed increased correspondingly with the flux of permeate as well as the salt rejection. The cast membrane of thin film attained a flux of permeate of 1.48 kg/(m^2·h) with 99.98 % salt rejection. Conversely, the electrospun nanofibrous membrane had better performance with a significantly higher permeate flux rate of 7.69 kg/(m^2·h) and an almost ideal salt rejection of 99.99 %.

Keywords: electrospinning, flat-sheet membrane, inversion phase, nanofibers, air gap membrane distillation

Introduction

Water shortage is a critical international issue that has gained attention for several decades [1]. This has severely affected biodiversity by threatening more than two-thirds of natural habitats. The World Health Organisation (WHO) predicts that by 2032, half of the world's population will face water scarcity [2]. As a result, safe drinking water has become rare. Global water reserves are around 1.4 billion km^3, with 97.5 % in seas and 2.5 % in fresh water from groundwater. Overall, only around 0.014 % is directly accessible to humans and other species. Desalination emerged as one of the most promising processes in the 21st century to obtain clean water from seawater and brackish water sources that can address the world's freshwater shortage and help meet global water demand [3].

There are currently two technologies that account for a large majority of the world's desalination capacity. Desalination can be broadly classified as either thermal or membrane

[1] Department of Chemical Engineering, College of Engineering, University of Baghdad, Al-Jaderia, Baghdad, Iraq, email: s.mirza1807@coeng.uobaghdad.edu.iq, ORCID: SM 0000-0003-4353-3192, BW 0000-0001-7842-5541
[*] Corresponding author: basmawaisi@coeng.uobaghdad.edu.iq

[4]. Thermal technologies have rarely been used for brackish water desalination; these processes need a significant amount of energy to produce the high heat of vaporisation of liquid water. As a result, determining how to handle the challenges of saltwater desalination and sewage treatment cost-effectively and in an energy-efficient manner has become the key to overcoming the problem of water shortage [5]. Membrane processes are now important in water treatment in many countries, because membrane separation has more advantages (this includes avoiding expensive and inefficient heat) than thermal technology [6]. Thus, researchers attempted to find a separation effective technique in the desalination process, which is termed membrane distillation technologies, or MD, a newly developing technique, a promising and alternative method for water desalination [7]. The advantages of MD desalination can be summarised by its tolerance to high salinity brine, working on low-grade temperature sources (less than 100 °C), 100 % salt rejection, and low fouling and low operating pressure (near atmospheric). But the main disadvantages of these processes are relatively low permeate flux [8-10]. MD processes have shown promising results in saltwater desalination, wastewater treatment, and many other applications, owing to the independence of the driving force from salinity.

Membrane Distillation (MD) is a separation process that utilises hydrophobic microporous membranes, which block liquid water from passing through their pores. Instead, only water vapour and volatile compounds are transported across the membrane, driven by a partial pressure difference between the feed and permeate sides [11]. In this manner, high-purity distillates can be obtained from various aqueous streams, including effluents from the textile and agri-food industries [12], waters contaminated by heavy metals [13], sea, and brackish waters [14]. The membrane influences water vapour flux, salt rejection, and distillate quality during seawater desalination. It has a considerable impact on the technological and economic efficiency of the MD process. Therefore, the selection of membrane material and pore size must be carefully suited to the individual application [15]. The wide range of membrane material applications, which include high hydrophobicity, low wettability, small thickness, low tortuosity, low thermal conductivity, and good chemical stability at membrane distillation's operating temperature, has made MD research for desalination applications more popular recently [16, 17], such polypropylene (PP) [18], polyvinylidene fluoride (PVDF) [19], and polytetrafluoroethylene (PTFE) [20].

The selection of a technique for polymer membrane fabrication depends on the choice of polymer and the desired structure of the membrane. Porous polymeric membranes can be created using several methods [21]. The most commonly used approaches in polymeric membrane fabrication include phase inversion [22], melt-spinning [23], cold-stretching (MSCS) [24], track etching [25], sintering [26], and electrospinning [27].

Among the various membrane fabrication methods, two stand out for their broad applicability across different fields: the conventional phase inversion technique and the more recent electrospinning method. Phase inversion is widely used due to its simplicity and ease of implementation, requiring relatively basic equipment. In this technique, a homogeneous polymer solution undergoes a controlled transformation from a liquid to a solid phase by immersion in a water bath. These characteristics make the processes relatively cost-effective. Moreover, they have been successfully applied to a wide range of materials. However, a significant drawback remains the toxicity of the solvents used. Additionally, incorporating organic or inorganic additives for antifouling purposes can lead to solubility issues, resulting in inhomogeneous dispersions within the membrane matrix.

This, in turn, reduces membrane stability and negatively impacts antifouling performance [28].

However, electrospinning is thought to be the best contemporary technique and the simplest way to create nanofiber deposits on a rotating disk after stretching the polymeric solution in an electrostatic field and evaporating the volatile solvent. High water contact angle, high surface roughness, high liquid entry pressure, high porosity, big surface area, and changeable pore size and thickness are some advantages of nanofiber membranes (ENMs) [29]. Thus, the electrospinning process can produce fibers with highly tunable properties, with the diameter of the electrospun fibers ranging from 10 nm to 100 μm [30]. Many studies have investigated and reported the preparation of polymeric membranes by phase inversion and electrospinning methods. The performance of flat-sheet poly (vinylidene fluoride-co-hexafluoropropylene) (PVDF-HFP) membrane was investigated experimentally and theoretically for water desalination in an air gap membrane distillation (AGMD) system. It was observed that increasing the feed temperature from 45 °C to 65 °C for a 35 g/L NaCl solution resulted in an approximately 3.8-fold increase in permeate flux. Additionally, increasing the feed flow rate from 0.25 L/min to 0.55 L/min led to a 30 % rise in flux. The rejection factor exceeded 99.9 %, while the permeate conductivity remained below 20 μS/cm [31]. With a maximum divergence of less than 20 %, the theoretical model findings were found to be in good agreement with the experimental data. For DCMD, a different team of researchers created a double-layer polyvinylidene fluoride-polymethyl methacrylate (PVDF-PMMA) membrane. Due to their intrinsic hydrophobicity, both polymers were tested in a DCMD arrangement under a range of operating circumstances. A membrane composition of 25 % wt. PVDF (lower layer) and 75 % wt. PMMA (top layer) resulted in a notable increase in water permeate flow, according to the study. This particular membrane composition produced a 99.757 % salt rejection rate and a flow of 44.192 kg/(m^2· h) [32].

In all these previous studies, all polymers used were synthetic and often derived from virgin materials. This study utilises recycled Perspex, a commonly used form of polymethyl methacrylate (PMMA), which offers both environmental and economic advantages. Perspex is a transparent thermoplastic frequently employed as a lightweight, shatter-resistant alternative to glass. Its insolubility and mechanical stability suggest strong potential for membrane fabrication. Moreover, recycling Perspex is significantly more cost-effective than sourcing new polymeric materials, making it a viable and sustainable option for membrane production. This research supports the advancement of a circular economy by promoting the reuse of post-consumer acrylic waste while simultaneously addressing the global demand for affordable and efficient materials in water treatment technologies.

This research aims to discuss and compare the desalination efficiency of the thin film polymeric membrane (prepared by the phase inversion method) and the nonwoven nanofibers polymeric membrane (prepared by the electrospinning method). The polymer used to prepare the membranes in this work was recycled acrylic (polymethyl methacrylate) (RA). The fabricated RA-based membranes were characterised using various analytical techniques, including Scanning Electron Microscopy (SEM), mechanical properties, water contact angle (WCA), and Fourier Transform Infrared Spectroscopy (FTIR). Then the membranes were applied for water desalination by the air gap membrane distillation (AGMD) process. Various parameters affecting membrane production, such as feed

temperature and modifications in the fabrication method under higher salt concentration solutions, were examined under continuous feed flow.

Materials and methods

Materials

In this study, waste acrylic hard plastic, specifically polymethyl methacrylate (PMMA), commonly known as Perspex, was utilised to prepare a recycled acrylic (RA) powder. Acrylic is technically classified as a type of glass due to its non-crystalline, vitreous structure and is widely used in applications such as casting resins, inks, coatings, and various industrial products. It was sourced from an advertising shop and was processed by grinding it into smaller fragments using an electric grinder to produce recycled acrylic (RA) powder. To optimise the fabrication process, phase inversion and electrospinning RA concentrations were used: 25 % wt. and 15 % wt. were selected, respectively, due to multiple preliminary attempts. These particular concentrations were dictated by the morphology demands of each process, for which the structural integrity of the dense membranes and the uniformity of the electrospun nanofibers were required. The organic solvents used to dissolve acrylic were N, N-Dimethylformamide (DMF) (density: 0.948 g/cm^3) and chloroform ($CHCl_3$) (density: 1.49 g/cm^3), which were supplied by Alfa Aesar. All chemical materials were used in their unique form without any additional modifications. Chloride-sodium (NaCl) (from Sigma-Aldrich) was used to prepare the brine solution. The distilled water was used as a coagulation bath in preparing the thin film membranes via the phase inversion method.

Membrane fabrication

In this work, the polymeric membranes were fabricated via two different preparation methods: the phase inversion method, producing a thin film membrane, and the electrospinning method, producing a nanofibers membrane. The thickness of both membrane types was fixed at approximately 300 µm and was determined by a digital Vernier.

Thin film membrane via phase inversion method

Polymeric solutions were prepared by dissolving the proper amount of 25 % wt. RA in 15 % wt. $CHCl_3$ first, then add the 60 % wt. DMF solvent using a magnetic stirrer at 500 rpm for 6 h, producing a clear and homogenous precursor polymeric solution. The flat sheet cast RA membrane was made using the phase inversion approach. The cast solution was poured over a clean glass. Then, a casting knife (Film applicator KTQ-II, Xiamen TOB New Energy Technology Co., Ltd., Fujian Province, China) was used to generate a 300 µm thin film layer on a purified glass plate. The membrane was then submerged in a water bath (precipitation bath) until it detached from the glass surface. The phase inversion process will result from the diffusion of a solvent and a nonsolvent across the interface between the nonsolvent (water) and the polymer casting solution. To ensure that all remaining solvent was eliminated from the membrane, the membranes were then left in the water bath for a full day.

Nonwoven nanofibers membranes via electrospinning system

The electrospinning (ES) is an innovative, cost-effective, simple, and economical membrane technology for nanofiber production, offering optimal control over the parameters of nanofibers that vary in size, shape, and doping [33]. The home-built electrospinning system was made of a syringe pump, a high-voltage power supply, and a rotating drum, as shown in our previous work [28]. The RA powder was dissolved at a concentration of 15 % wt. in a specific amount of 15 % wt. $CHCl_3$ solvent first, then the 70 % wt. DMF solvent was added using a magnetic stirrer at 500 rpm at room temperature for 5 h. The mixing process continued until the solution became clear and homogeneous. To prevent needle clogging and to obtain defect-free RA-based nanofibers, the prepared precursor should have low viscosity; thus, the RA polymer concentration was only 15 % wt., which is good enough to be spinnable.

The obtained homogenous precursor solution was transferred to a 5 mL plastic syringe fitted with a capillary metal 21-gauge needle. The polymeric solution was pumped at a rate of 2 mL/h with a tip-to-collector distance of 13 cm. The electrospinning process was carried out at room temperature with a relative humidity of 20 %. The polymer solution was exposed to a strong electrostatic force (18 kV). The polymer jet was ejected and collected on a revolving drum. The solvent then evaporated, forming a mat of nonwoven nanofibers on the collector's surface to generate a 300 µm [34]. After electrospinning, the dried membranes were then stored in clean plastic containers.

Characterisation of membranes

Scanning electron microscopy (SEM)

A scanning electron microscope (SEM) is a widely used research tool that produces images of a sample by scanning it with a focused beam of electrons (Thermo Fisher Scientific, FEI Quanta 200, USA). SEM images provide valuable information about the surface topography and the pore size distribution of both prepared RA-based membranes. An image algorithm was developed to measure the feature pore size distribution from the SEM images by analysing the pore sizes of each membrane sample using Image J software and the obtained images (National Institutes of Health, USA).

The membrane porosity

The porosity of a membrane is a crucial determining factor for the separation performance of membranes. Membrane porosity indicates the void volume fraction and is defined as the volume of the pores divided by the total volume of the membrane [35]. To determine membrane porosity using the gravimetric method, each membrane sample was weighed and soaked in alcohol for 30 minutes. The samples' dry and wet weights were recorded before and after alcohol immersion, respectively. Then the porosity, ε, was calculated using the equation [33]:

$$\varepsilon = \frac{W_w - W_d}{A \cdot \delta \cdot \rho_l} \tag{1}$$

where W_w and W_d are wet and dry membrane mass [g], A is membrane area [cm²], δ is membrane thickness [cm], and ρ_l is alcohol density at room temperature [g/cm^3].

Contact angle

The wettability of the surface membranes was assessed through contact angle measurements using an optical contact angle meter (CAM 110-04w) by dropping perpendicularly onto the surface of the membrane. In this method, a drop of distilled water was deposited on a piece of membrane. After that, in a stationary state, the camera in the device captured an image of the droplet, the CA was automatically determined by the software.

Fourier-transform infrared spectroscopy (FTIR)

Fourier-transform infrared spectroscopy (FTIR) (Spectrum 1800, Shimadzu, Japan) makes infrared spectroscopy used to identify the chemical structure and functional groups present in the membranes by passing radiation through a sample. The sample absorbs a portion of the infrared light, while the remainder is transmitted. The resultant spectrum indicates molecule absorption and transmission, creating a molecular fingerprint of the sample, and operating in the 4000 cm^{-1} - 400 cm^{-1} wavenumber range [34].

Mechanical properties

The mechanical properties of membranes are a crucial material characteristic for practical applications, affecting factors such as reusability, handling, and resistance to deformation [36]. Using a Dynamic Mechanical Analyser (DMA) (AG-A10T, Shimadzu, Japan), the breaking strength and Young's modulus of the membranes were measured in order to evaluate their mechanical properties. At 25 °C and room humidity, specimens with dimensions of 10 cm in length and 1 cm in width were assessed. The stress-to-strain ratio is the definition of Young's modulus, a metric used to quantify a material's elasticity [37, 38].

Evaluation of the membrane performance in air gap membrane distillation (AGMD) system

One of four typical arrangements of MD is Air Gap Membrane Distillation (AGMD); the schematic and digital model of the process are presented in Figures 1 and 2, respectively. The feed solution was heated by the heater (water bath), and a pump circulated water through the top part of the membrane piece. The flow rate is regulated by a control valve and monitored by a pressure gauge. Coolant flows through the bottom (chiller), managed by a control valve with a pressure gauge, and the generated permeate is collected in the middle chamber and gathered in a measuring cylinder. Within the membrane module, both the feed solution and the coolant are pumped in a closed-loop system with counter-current flow. The membrane is located between the feed and air gap compartments, and the vaporised water passes via a stagnant air gap between the membrane and a condenser plate. The inlet and outlet temperatures of the feed water and coolant were continually measured by four sensors placed at the inlets and outlets of each side of the membrane module. AGMD's flat sheet membrane module was designed and constructed from acrylic panels (Perspex) that are chemically resistant, have high heat transfer resistance, and are easy to fabricate. The chamber side in the AGMD configuration has a thickness of 1.5 cm, a length of 7 cm, and a width of 7 cm.

Fig. 1. Image of air gap membrane distillation configuration

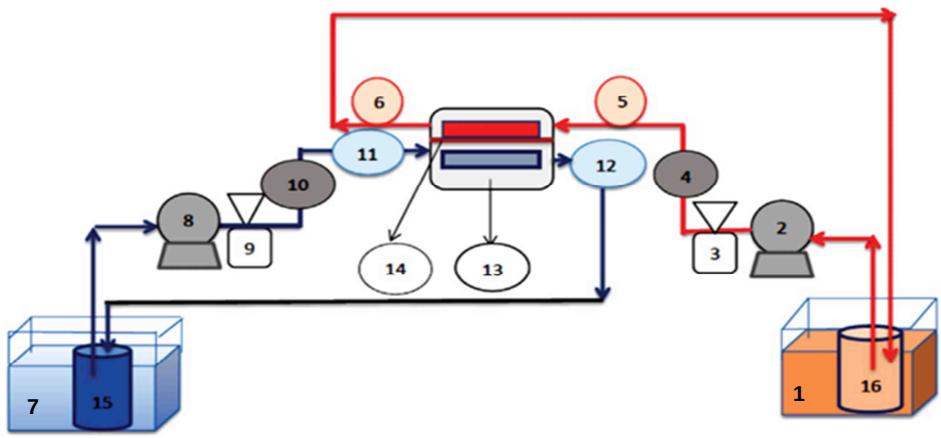

(1)	Bath for feed	(2)	Pump for feed
(3)	Rotameter for feed	(5,6)	Sensors to measure the temperature inlet and outlet (bath)
(7)	Chiller for permeate mm	(11,12)	Sensors to measure the temperature inlet and outlet (chiller)
(8)	Pump for chiller (permeate)	(9)	Rotameter for chiller (permeate)
(4)	pressure gauge for inlet feed (bath)	(10)	pressure gauge for inlet (chiller)
(15,16)	Tank for permeate and Tank for feed	(13,14)	Membrane module and Membrane

Fig. 2. The schematic diagram layout of the experimental design in measuring the performance of the membrane in the AGMD process [33]

AGMD tests were run for 3 h for each experimental condition. The salt concentrations of the feed and permeate into and out of the membrane module were precisely measured using a commercial digital meter (Handheld TDS EC pH temp salinity meter). In the AGMD process, the measurements of the collected volume of the permeate flux were determined by the continuous change in the volume of the permeate distilled water in the

vessels. Permeate flux, J [kg/(m^2·h)], was used to assess the performance for each MD configuration. It was calculated using the equation [39]:

$$J = \frac{V \cdot \rho_w}{A \cdot t} \tag{2}$$

where V is the freshwater volume [L], ρ_w is the water density [kg/L], t is the operational time [h], and A is the area of the membrane and salt rejection, SR [%] as given in the equation [40]:

$$SR = \frac{C_1 - C_2}{C_1} \cdot 100 \tag{3}$$

where SR is the salt retention, C_1 is the feed concentration, and C_2 is the concentration of the permeate [41].

For reproducibility, each experiment in this process was repeated at least three times, and the average values of water flux and salt rejection were reported.

Results and discussion

Membranes characterisations

Figure 3 presents the SEM image of the surface morphology and the corresponding pore size distribution of both prepared membranes. Figure 3a shows the surface analysis of the thin film cast 25 % wt. RA-based membrane prepared. It shows a rough surface composite that contains regular circular pore-like structures and has homogeneously distributed moderately sized pores that contain more open pores to the surface with some spores dispersed across it. The SEM image reveals that the average pore size distribution was estimated to be 0.38 µm, based on pores measurements using ImageJ. The major percentage of the pore size is less than 1 µm due to the structure of a dense membrane surface because of the high polymer RA concentration in the precursor solution [42], which is typical for membranes designed for high salt rejection, high selectivity, and mechanical stability in the MD process.

The surface morphology and the corresponding pore size distribution of the fabricated 15% wt. RA-based nanofiber membrane via the electrospinning method is shown in Figure 3b. The samples obtained showed that many pores are sparse on the top surface of the membrane. The SEM image reveals that the average pore size distribution was estimated to be 2.2 µm, based on measurements of ImageJ. The pore size distribution indicates consistent formation ranging between 0.5 µm to 5 µm, which is a relatively broad distribution that is useful for mass transfer in membrane distillation (MD) applications because fine fiber dimensions contribute to a high surface-area-to-volume ratio. Additionally, the absence of beads and surface defects indicates a stable electrospinning process resulting in homogeneous fiber formation.

The most interesting element that influences membrane performance in MD applications is pore size; the holes should be big enough to accelerate the necessary mass flux. However, the membrane had a rather high porosity, which was due to the linked fiber structure and the existence of voids [43]. As a result, fibrous networks offer adequate mechanical support while maintaining a high level of hydrophobicity, which is crucial for sustaining liquid-vapour separation under AGMD working conditions. Compared to the thin film cast membrane, this surface is anticipated to contribute to higher vapour flow.

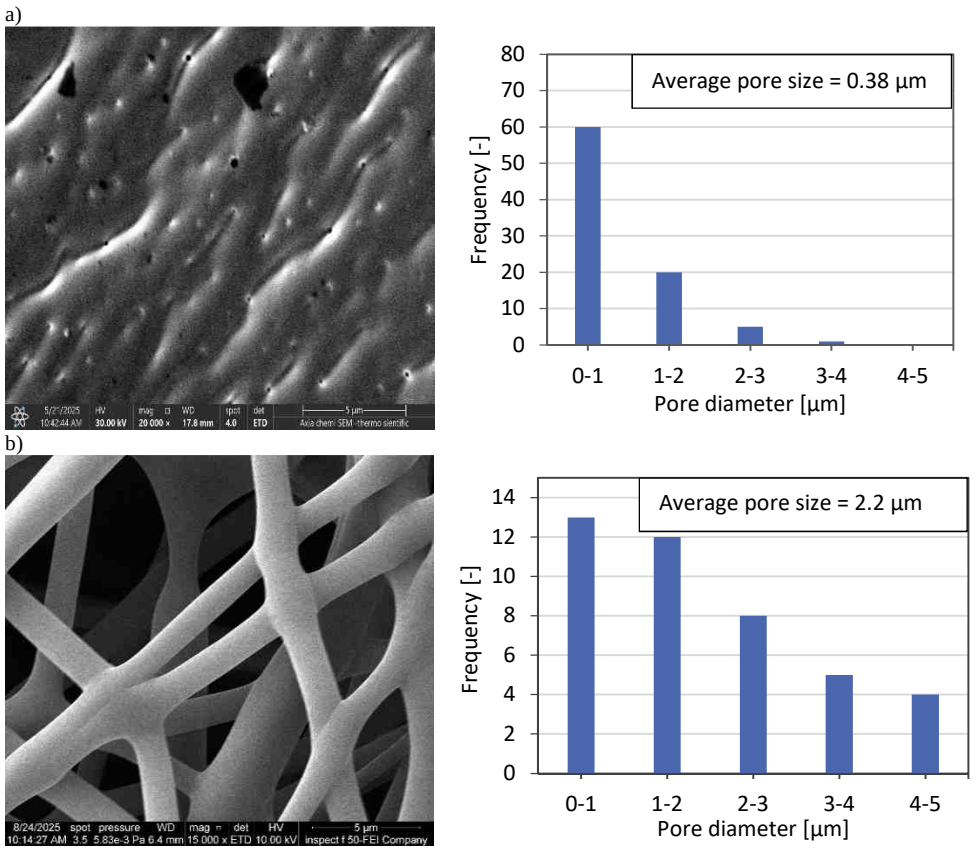

Fig. 3. The surface morphology and the corresponding pore size distribution of the prepared membranes: a) RA-based thin film membrane via phase inversion method, b) RA-based nanofibers membrane via electrospinning method

The measured porosity of the prepared RA-based cast thin film membrane was 73.52 %, indicating a dense and compact membrane structure with few voids. This morphology limits the vapour transport but helps to improve mechanical stability. Similar results have been reported [44], where increasing the concentration of RA-based increased the viscosity of the casting solution, which reduces porosity. While the recorded porosity of the prepared electrospun nanofiber membrane was 93.52 %, the ultrafine nanofiber net becomes highly porous to create a large amount of empty space, which increases the permeability of the membrane, and at low polymer concentration, the membrane permeability is significantly high. The porosity increases signify a decrease in the mean fiber diameter and consequently imply that the spinning solution would be less viscous. Thus, achieving adequate porosity is very important in order to have the proper balance of high vapour flux, wetting resistance and mechanical stability. Additionally, the contact angle measurement of a water droplet (WCA) on the membrane surface. The membrane made by using the thin-film casting technique using RA had a WCA of 82.47°. On the contrary, the nanofiber membrane by the electrospun method showed a much higher WCA

of 121.85° which denotes a highly hydrophobic surface. This hydrophobic property is especially beneficial in the application of (MD) since it avoids wetting the pores, and only water vapour is able to diffuse through the membrane. The significant comparison between the two fabrication techniques, electrospinning and phase inversion (casting), serves to emphasise the effect of the architectural features of surfaces on wettability [42]. According to the literature, the angle of contact depends not only on the intrinsic characteristics of the polymer but also on other essential parameters, such as the roughness of the surface, the distribution of pore sizes, and the heterogeneity of the surface [45].

Displayed in Figure 4a, the spectra show typical peaks at 2848.86 cm^{-1}, 2922.16 cm^{-1}, and 3024 cm^{-1}, which are present in all RA membranes. These peaks indicate the presence of the are attributed to alkenic C–H stretching vibrations. Additional peaks at 3414.00 cm^{-1} and 3468.01 cm^{-1} were assigned to O–H stretching [46]. A characteristic stretching vibration prominent peak at 1635.64 cm^{-1}, along with the broader range from 1450.47 cm^{-1} to 1620.21 cm^{-1}, represents the C=O stretching vibration of ester [47], confirming the presence of acrylic components in the nanofiber membrane. The bending vibrations of CH_2 and CH_3 groups are evident at 1450.47 cm^{-1} and 1369.46 cm^{-1}, respectively. In the 1325.10 cm^{-1} - 1028 cm^{-1} region, multiple peaks correspond to C–O–C stretching vibrations of the ester moiety. Additionally, peaks in the 840 cm^{-1} - 750 cm^{-1} region (including 754.17 cm^{-1} and 698.23 cm^{-1}) are associated with out-of-plane bending of $–CH_2$ groups or side-chain vibrations.

The chemical composition of developed membranes was investigated by the FTIR spectrum (Fig. 4b), which displays characteristic absorption bands that confirm the chemical structure of electrospun PMMA. The peaks observed at 3022.45 cm^{-1} - 3057.17 cm^{-1} are attributed to alkenic C–H stretching vibrations [48]. While the strong absorptions in the 2920.23 cm^{-1} - 2848.86 cm^{-1} range correspond to C–H stretching of $–CH_3$ and $–CH_3–$ groups, consistent with the aliphatic backbone of PMMA. A prominent peak at 1743.65 cm^{-1}, along with the broader range from 1645.28 cm^{-1} to 1940.39 cm^{-1}, represents the C=O stretching vibration of ester groups, confirming the presence of acrylic components in the nanofiber membrane [49]. The bending vibrations of CH_2 and CH_3 groups are evident at 1490.97 cm^{-1} and 1371.39 cm^{-1}, respectively. In the 1325.10 cm^{-1} - 1000 cm^{-1} region, multiple peaks correspond to C–O–C stretching vibrations of the ester moiety. Additionally, peaks in the 840 cm^{-1} - 600 cm^{-1} region (including 756.1 cm^{-1} and 698.3 cm^{-1}) are associated with out-of-plane bending of $–CH_2$ groups or side-chain vibrations. Collectively, these spectral features confirm the successful synthesis of PMMA nanofibers with intact ester functionalities and indicate the high chemical purity of the electrospun membrane, as no significant signals of degradation or contamination were detected.

The mechanical characteristics of electrospun fibers are greatly affected by fiber alignment within the membrane. Electrospun recycled acrylic (RA) membranes demonstrated outstanding elongation rates, with tensile strengths of 0.0624 MPa for aligned, random, and bi-layered topologies, respectively. The SEM micrographs of random membranes reveal fiber fusion, a mechanism that presumably enhances Young's modulus while increasing elasticity. These findings are promising, as they offer a viable alternative to overcome the common limited inflexibility of cast membranes. The lack of flexibility in cast membranes is due to the solvent phase inversion fabrication method, according to 17.22 MPa, which typically does not use plasticisers. Unlike electrospun membranes, cast films exhibit poorer fiber orientation and reduced stretchability under mechanical stress.

Typically, penetrant polymer networks reduce cohesive intermolecular forces among polymer chains, affecting mechanical strength, as shown in Figure 5. Mechanical strength is critical for preserving membrane structural integrity throughout transport, installation, and operation. A strong membrane is less susceptible to damage during handling, lowering the chance of flaws that might compromise performance. Good mechanical qualities guarantee that membrane distillation (MD) membranes are resilient and long-lasting, thereby increasing their efficacy in water purification applications.

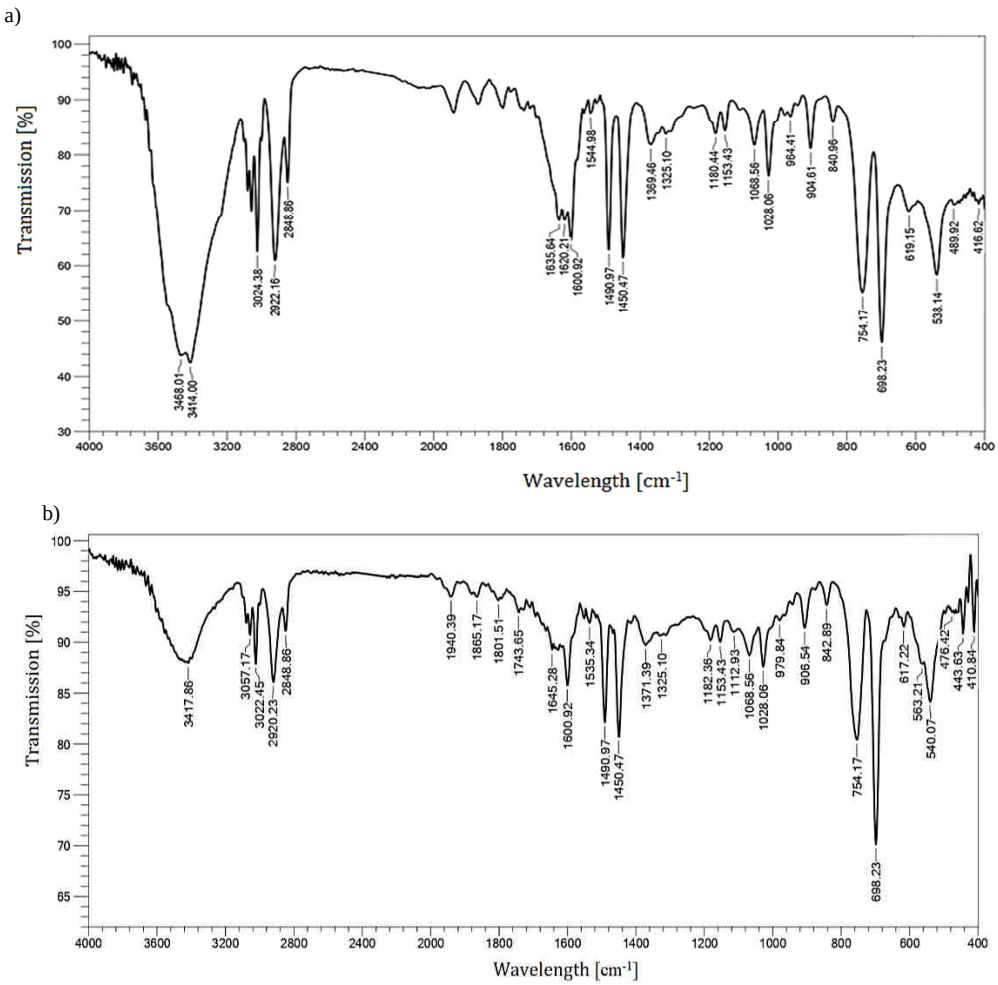

Fig. 4. The FTIR spectra of the RA-based membrane fabricated by: a) the phase inversion method, b) the electrospinning method

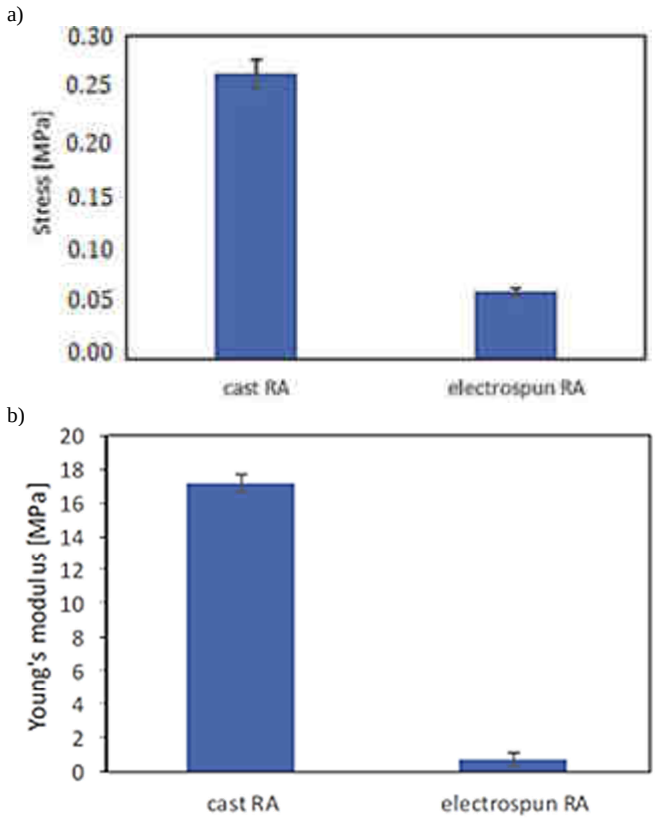

Fig. 5. The mechanical properties of the RA-based thin film-casted membrane and the nanofiber membrane: a) Breaking strength, b) Young's modulus

Table 1

Comparison of membrane characterisation of the fabricated membranes via phase inversion and electrospun methods

Membranes characterisations	Phase inversion	Electrospinning
Thickness [μm]	300	300
Average pore size [μm]	0.38	2.2
Porosity [%]	73.52	93.59
Contact angle [°]	82.47	121.85
Young's modulus [MPa]	17.22 ± 0.35	0.74 ± 0.08

Membrane performance test

The AGMD system was created to get experimental data to evaluate the potential of the fabricated membranes for brine water desalination. The study investigated the effects of operating parameters, including feed water temperature, which is the most critical parameter influencing membrane distillation performance. The cold-side temperature of 15 °C and flow rate of 0.3 L/min were maintained constant at a brine concentration of

35 g/L, a membrane thickness of 13 mm, an air gap thickness of 6 mm, and the feed flow rate was almost 0.3 L/min.

The influence of feed temperature on permeate flux was examined under controlled conditions of the two membranes; the feed temperature was varied from 45 °C to 65 °C, while all other parameters remained constant. The properties and separation performance of the two types of fabricated membranes were compared and summarised in Table 2. It presented the corresponding permeate flux and salt rejection values at each feed temperature.

Table 2

Comparison of the feed temperature influence on the fabricated membranes via phase inversion and electrospinning fabrication methods

Temperature [°C]	Phase inversion		Electrospinning	
	Permeate flux [kg/(m^2·h)]	Salt rejection [%]	Permeate flux [kg/(m^2·h)]	Salt rejection [%]
45	0.960	98.978	4.396	99.997
55	1.185	98.988	5.495	99.998
65	1.480	99.989	7.692	99.999

When the feed temperature increased from 45 °C to 65 °C, the permeate flux increased from 0.960 kg/(m^2· h) to 1.480 kg/(m^2· h) for the RA-based cast membranes and from 4.396 kg/(m^2· h) to 7.692 kg/(m^2· h) for the nanofiber's membrane. The observed increase in the membrane performance with increasing temperature is expected because higher temperatures significantly increase the saturated vapour pressure of water, thereby enhancing the driving force for vapour transport across the membrane in the membrane distillation (MD) process. This relationship is described by the Antoine equation, which explains how vapour pressure rises with temperature, an essential factor governing mass transfer in MD processes [50].

When comparing the properties of the two membranes, the enhanced flux observed for the 15 % wt. RA nanofiber membrane can be primarily attributed to its higher hydrophobicity, as evidenced by a water contact angle of 121°. The improved mass transfer is further associated with the highly porous and interconnected nanofibrous structure, which provides continuous vapour transport pathways and effectively minimises the occurrence of partial wetting. In addition, the relatively large pore size, approximately 2.2 μm, contributes significantly to the increased flux performance. In contrast, the 25 % wt. RA cast membrane exhibited a lower water contact angle of 82°. The increased RA concentration led to higher viscosity of the casting solution, which in turn reduced membrane porosity and resulted in a smaller mean pore radius of approximately 0.38 μm. Despite the lower hydrophobicity, no wetting phenomena were observed during the experimental tests, indicating that the membrane maintains a certain level of resistance against water penetration through its surface microstructure.

However, an increase in feed temperature resulted in a significant enhancement of permeate flux; this improvement must be carefully weighed against the corresponding rise in energy consumption required to heat the feed solution. Although this thermal gain entails higher energy input, particularly at temperatures exceeding 60 °C, where heating demands become more substantial [51]. Thus, the maximum flux was achieved at 65 °C; the selection of this temperature as the optimal operating condition in this study also considered its practical applicability in real-world desalination systems and an effective compromise

between performance and energy efficiency, delivering high water recovery while maintaining a relatively reasonable thermal energy requirement. Therefore, it supports its suitability for efficient brine treatment using AGMD technology. Despite temperature variations, the membrane consistently exhibited excellent desalination performance. Comparing the retention characteristics of the RA electrospun and cast membranes at 65 ℃ revealed rejection values of 98.978 % and 99.989 %, respectively, as shown in Figure 6.

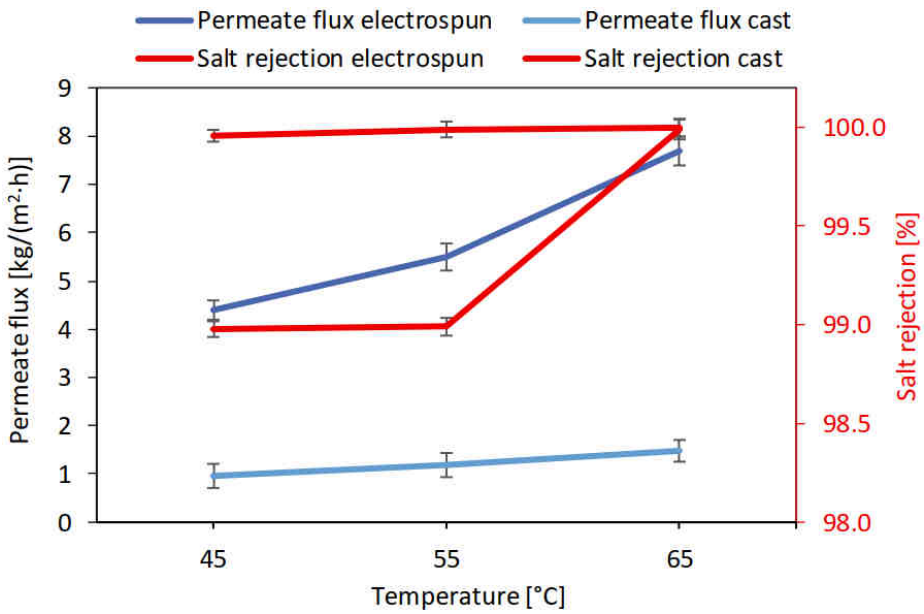

Fig. 6. Comparison between phase inversion and electrospinning from the study of the influence of feed temperature on the permeation flux and rejection at 0.3 L/min, 6 mm, and 35 g/L NaCl

Conclusion

This paper has compared two methods of membrane fabrication, namely electrospinning and phase inversion, at different concentrations (15 % wt. and 25 % wt.) using recycled acrylic (RA) as a sustainable polymer source for use in Air Gap Membrane Distillation (AGMD) applications. The concentration of the precursor solution plays a crucial role in determining an increase in roughness for both types of membranes. The membranes' nanofibers exhibited favourable morphological and physicochemical properties, including a highly porous and uniform fiber network (confirmed by SEM), significant surface roughness (AFM), and strong hydrophobicity (contact angle > 121°), while it tends to increase hydrophilicity for the cast membranes (82.47°), confirmed by the contact angle test. This is also the case in the porosity, where the electrospun nanofiber membrane was found to have a decrease, whilst the cast membrane had an increase. Both membranes' FTIR analysis confirmed the preservation of functional groups, ensuring chemical integrity and thermal stability. The membranes were evaluated in a custom-designed AGMD setup under operational conditions, including changing feed temperatures (45 °C - 65 °C). In terms of performance, electrospun recycled acrylic (RA)

nanofiber membranes exhibited a flux of 7.692 kg/($m^2 \cdot$ h) and a salt rejection rate exceeding 99.99 %, outperforming cast RA membranes. These membranes showed good performance in terms of salt rejection/water flux, and the best part is they could be operated without pressure. Therefore, a more cost-effective method is the electrospinning process that is pressure-free. In addition, the distinctive characteristics of electrospun nanofiber membranes make them highly promising for industrial applications, especially in the treatment of saline wastewater. Nevertheless, the following research deserves to be carried out in order to produce large-scale electrospun membranes and carry out tests in large-scale facilities and evaluate their viability in the industry comprehensively. The results verify the fact that RA-based nanofiber membranes are not only beneficial to the environment but also extremely efficient in the desalination of high-salinity brine using AGMD. This work contributes to the development of cost-effective and sustainable membrane materials for future water treatment technologies.

References

[1] Shawish AA, Nabhan T, Almadidy A. Potable water in UAE: An overview of water characteristics and sources of contamination. J Environ Toxicol Stud. 2019;3(2):1-4. DOI: 10.16966/2576-6430.120.

[2] World Health Organization. Progress on Household Drinking Water, Sanitation and Hygiene 2000-2024: Special Focus on Inequalities. World Health Organization; ISBN: 9240115145.

[3] Shemer H, Wald S, Semiat R. Challenges and solutions for global water scarcity. Membranes. 2023;13(6):612. DOI: 10.3390/membranes13060612.

[4] Curto D, Franzitta V, Guercio A. A review of the water desalination technologies. Appl Sci. 2021;11(2):670. DOI: 10.3390/app11020670.

[5] Feria-Díaz JJ, López-Méndez MC, Rodríguez-Miranda JP, Sandoval-Herazo LC, Correa-Mahecha F. Commercial thermal technologies for desalination of water from renewable energies: a state of the art review. Processes. 2021;9(2):262. DOI: 10.3390/pr9020262.

[6] Zhou Y, Chen L, Huang M, Hu W, Chen G, Wu B. Experimental investigation of the desalination process for direct contact membrane distillation using plate and frame membrane module. Appl Sci. 2023;13(16):9439. DOI: 10.3390/app13169439.

[7] Drioli E, Ali A, Macedonio F. Membrane distillation: Recent developments and perspectives. Desalination. 2015;356:56-84. DOI: 10.1016/j.desal.2014.10.028.

[8] Elmarghany MR, El-Shazly AH, Salem MS, Sabry MN, Nady N. Thermal analysis evaluation of direct contact membrane distillation system. Case Stud Thermal Eng. 2019;13:100377. DOI: 10.1016/j.csite.2018.100377.

[9] Safi NN, Waisi BI. Enhanced hydrophobic double-layer nanofibers membranes for direct contact membrane distillation. Ecol Eng Environ Technol. 2024;25:325-35. DOI: 10.12912/27197050/184224.

[10] Alkarbouly SM, Waisi BI. Fabrication of electrospun nanofibers membrane for emulsified oil removal from oily wastewater, Baghdad Sci J. 2022;19(6):1238-48. DOI: 10.21123/bsj.2022.6421.

[11] Criscuoli A. Membrane distillation process. Membranes. 2021;11(2):144. DOI: 10.3390/membranes11020144.

[12] Papaioannou EH, Mazzei R, Bazzarelli F, Piacentini E, Giannakopoulos V, Roberts MR, Giorno L. Agri-food industry waste as resource of chemicals: The role of membrane technology in their sustainable recycling. Sustainability. 2022;14(3):1483. DOI: 10.3390/su14031483.

[13] Yarlagadda S, Gude VG, Camacho LM, Pinappu S, Deng S. Potable water recovery from As, U, and F contaminated ground waters by direct contact membrane distillation process. J Hazard Mater. 2011;192(3):1388-94. DOI: 10.1016/j.jhazmat.2011.06.056.

[14] Politano A, Argurio P, Di Profio G, Sanna V, Cupolillo A, Chakraborty S, et al. Photothermal membrane distillation for seawater desalination. Adv Mater. 2016;29(2):1603504. DOI: 10.1002/adma.201603504.

[15] Lalia BS, Kochkodan V, Hashaikeh R, Hilal N. A review on membrane fabrication: Structure, properties and performance relationship. Desalination. 2013;326:77-95. DOI: 10.1016/j.desal.2013.06.016.

[16] Xu J, Singh YB, Amy GL, Ghaffour N. Effect of operating parameters and membrane characteristics on air gap membrane distillation performance for the treatment of highly saline water. J Membrane Sci. 2016;512:73-82. DOI: 10.1016/j.memsci.2016.04.010.

[17] Manawi Y, Jawad J, Hussain A, Aljlil S, Lawler J, Kochkodan V. Enhancement of membrane distillation performance by porous organic and inorganic materials: a state-of-the-art review. Appl Water Sci. 2025;15(6):117. DOI: 10.1007/s13201-025-02449-7
[18] Fang J, Zhang L, Sutton D, Wang X, Lin T. Needleless melt-electrospinning of polypropylene nanofibres. J Nanomater. 2012;2012(1):382639. DOI: 10.1155/2012/382639.
[19] Albiladi A, Gzara L, Organji H, Alkayal NS, Figoli A. Electrospun poly (vinylidene fluoride-co-hexafluoropropylene) nanofiber membranes for brine treatment via membrane distillation. Polymers. 2023;15(12):2706. DOI: 10.3390/polym15122706.
[20] Defor C, Chou SF. Electrospun polytetrafluoroethylene (PTFE) fibers in membrane distillation applications. AIMS Materials Sci. 2024;11(6):1179-98. DOI: 10.3934/MATERSCI.2024058.
[21] Tan X, Rodrigue D. A review on porous polymeric membrane preparation. Part II: Production techniques with polyethylene, polydimethylsiloxane, polypropylene, polyimide, and polytetrafluoroethylene. Polymers. 2019;11(8):1310. DOI: 10.3390/polym11081310.
[22] Mansourizadeh A, Ismail AF, Abdullah MS, Ng BC. Preparation of polyvinylidene fluoride hollow fiber membranes for CO_2 absorption using phase-inversion promoter additives. J Membrane Sci. 2010;35(1-2):200-7. DOI: 10.1016/j.memsci.2010.03.031.
[23] Zhong D, Zhou J, Wang Y. Hollow-fiber membranes of block copolymers by melt spinning and selective swelling. J Membrane Sci. 2021;632:119374. DOI: 10.1016/j.memsci.2021.119374.
[24] Komaladewi AA, Aryanti PT, Lugito G, Surata IW, Wenten IG. Recent progress in microfiltration polypropylene membrane fabrication by stretching method. In E3S Web Conf. 2018;67:03018. DOI: 10.1051/e3sconf/20186703018.
[25] Apel P. Track etching technique in membrane technology. Radiation Measurements. 2001;34(1-6):559-66. DOI: 10.1016/S1350-4487(01)00228-1.
[26] Monash P, Pugazhenthi G, Saravanan P. Various fabrication methods of porous ceramic supports for membrane applications. Rev Chem Eng. 2013;29(5):357-83. DOI: 10.1515/revce-2013-0006.
[27] Al-Okaidy HS, Waisi BI. The effect of electrospinning parameters on morphological and mechanical properties of PAN-based nanofibers membrane. Baghdad Sci J. 2023;20(4):1433. DOI: 10.21123/bsj.2023.7309.
[28] Geleta TA, Maggay IV, Chang Y, Venault A. Recent advances on the fabrication of antifouling phase-inversion membranes by physical blending modification method. Membranes. 2023;13(1):58. DOI: 10.3390/membranes13010058.
[29] Prasanna NS, Choudhary N, Singh N, Raghavarao KS. Omniphobic membranes in membrane distillation for desalination applications: A mini-review. Chem Eng J Adv. 2023;14:100486. DOI: 10.1016/j.ceja.2023.100486.
[30] Nasreen SA, Sundarrajan S, Nizar SA, Balamurugan R, Ramakrishna S. Advancement in electrospun nanofibrous membranes modification and their application in water treatment. Membranes. 2013;3(4):266-84. DOI: 10.3390/membranes3040266.
[31] Alsalhy QF, Ibrahim SS, Hashim FA. Experimental and theoretical investigation of air gap membrane distillation process for water desalination. Chem Eng Res Design. 2018;130:95-108. DOI: 10.1016/j.cherd.2017.12.013.
[32] Safi NN, Waisi BI. Preparation of electrospun double-layer PVDF: PMMA membrane non-woven nanofibers for desalination by membrane distillation process. Desalin Water Treat. 2023;314:49-58. DOI: 10.5004/dwt.2023.30063.
[33] Sabeeh H, Waisi BI. Effect of solvent type on PAN-based nonwoven nanofibers membranes characterizations. Iraqi J Chem Petroleum Eng. 2022;23(4):43-8. DOI: 10.31699/ijcpe.2022.4.6.
[34] Coates J. Interpretation of Infrared Spectra, a Practical Approach. In: Meyers RA, McKelvy ML, editors. Encyclopedia of Analytical Chemistry. Chichester; John Wiley Sons Ltd.: 2000. 10815-37. DOI: 10.1002/9780470027318.a5606.
[35] Tooma MA, Najim TS, Alsalhy QF, Marino T, Criscuoli A, Giorno L, et al. Modification of polyvinyl chloride (PVC) membrane for vacuum membrane distillation (VMD) application. Desalination. 2015;373:58-70. DOI: 10.1016/j.desal.2015.07.008.
[36] Naseeb N, Mohammed AA, Laoui T, Khan Z. A novel PAN-GO-SiO_2 hybrid membrane for separating oil and water from emulsified mixture. Materials. 2019;12(2):212. DOI: 10.3390/ma12020212.
[37] Rabiei M, Palevicius A, Dashti A, Nasiri S, Monshi A, Vilkauskas A, et al. Measurement modulus of elasticity related to the atomic density of planes in unit cell of crystal lattices. Materials. 2020;13(19):4380. DOI: 10.3390/ma13194380.
[38] Greiner A, Wendorff JH. Electrospinning: a fascinating method for the preparation of ultrathin fibers. Angewandte Chemie Int Ed. 2007;46(30):5670-703. DOI: 10.1002/anie.200604646.

[39] Al-Harby NF, El Batouti M, Elewa MM. A comparative analysis of pervaporation and membrane distillation techniques for desalination utilising the sweeping air methodology with novel and economical pervaporation membranes. Polymers. 2023;15(21):4237. DOI: 10.3390/polym15214237.
[40] Irfan M, Basri H, Irfan M. An experimental investigation: effect of phase inversion methods on membrane structure and its performance on PEG filtration. J Appl Membrane Sci Technol. 2015;17(1). DOI: 10.11113/amst.v17i1.11.
[41] Hardikar M, Felix V, Presson LK, Rabe AB, Ikner LA, Hickenbottom KL, et al. Pore flow and solute rejection in pilot-scale air-gap membrane distillation. J Membrane Sci. 2023;676:121544. DOI: 10.1016/j.memsci.2023.121544.
[42] Diwan T, Abudi ZN, Al-Furaiji MH, Nijmeijer A. A competitive study using electrospinning and phase inversion to prepare polymeric membranes for oil removal. Membranes. 2023;13(5):474. DOI: 10.3390/membranes13050474.
[43] Waisi BI. Carbonized copolymers nonwoven nanofibers composite: surface morphology and fibers orientation. Iraqi J Chem Petroleum Eng. 2019;20(2):11-5. DOI: 10.31699/IJCPE.2019.2.2.
[44] Nayab SS, Abbas MA, Mushtaq S, Khan Niazi B, Batool M, Shehnaz G, et al. Anti-foulant ultrafiltration polymer composite membranes incorporated with composite activated carbon/chitosan and activated carbon/thiolated chitosan with enhanced hydrophilicity. Membranes. 2021;11(11):827. DOI: 10.3390/membranes11110827.
[45] Ali I, Bamaga OA, Gzara L, Bassyouni M, Abdel-Aziz MH, Soliman MF, et al. Assessment of blend PVDF membranes, and the effect of polymer concentration and blend composition. Membranes. 2018;8(1):13. DOI: 10.3390/membranes8010013.
[46] Pasieczna-Patkowska S, Cichy M, Flieger J. Application of Fourier transform infrared (FTIR) spectroscopy in characterization of green synthesized nanoparticles. Molecules. 2025;30(3):684. DOI: 10.3390/molecules30030684.
[47] Tayal E, Chandran AM, Mural PK. A comparative study of cellulose acetate/polycaprolactone blend electrospun and phase-inversion membranes for forward osmosis. Proc Yukthi. Govt Eng College Kozhikode. 2021. DOI: 10.2139/ssrn.4022530.
[48] Kavipriya R, Kavitha HP, Karthikeyan B, Nataraj A. Molecular structure, spectroscopic (FT-IR, FT-Raman), NBO analysis of N, N′-diphenyl-6-piperidin-1-yl-[1, 3, 5]-triazine-2, 4-diamine. Spectrochim Acta Part A: Molec Biomolec Spectroscopy. 2015;150:476-87. DOI: 10.1016/j.saa.2015.05.052.
[49] Tan SJ, Supri AG, Foo KL, Al Bakri AM, Liew YM, Heah CY. Effect of poly(methyl methacrylate) (PMMA) on tensile properties and spectroscopy infrared (FTIR) characteristics of LDPE/WHF composites. Appl Mechanics Materials. 2015;815:101-5. DOI: 10.4028/www.scientific.net/AMM.815.101.
[50] Moshele P, Stenzel MR, Drolet D, Arnold SF. Comparing Antoine parameter sources for accurate vapor pressure prediction across a range of temperatures. Annals Work Exposures Health. 2024;68(4):409-19. DOI: 10.1093/annweh/wxae010.
[51] Al-Sairfi H, Koshuriyan MZ, Ahmed M. Performance feasibility study of direct contact membrane distillation systems in the treatment of seawater and oilfield-produced brine: the effect of hot-and cold-channel depth. Desalin Water Treat. 2023;313:26-36. DOI: 10.5004/dwt.2023.29942.